

Modeling and Effects of Various Drying Methods on Sweet Potato Starch Properties

Ho Minh THAO¹ and Athapol NOOMHORM²

¹Food Technology Department, An Giang University, An Giang 94000, Vietnam

²Food Engineering and Bioprocess Technology, School of Environment Resources and Development, Asian Institute of Technology, Pathumthani 12120, Thailand

(Corresponding author; e-mail: hmthao@agu.edu.vn)

Received: 8 August 2011, Revised: 6 November 2011, Accepted: 16 November 2011

Abstract

Eleven mathematical models (Lewis, Page, Henderson and Pabis, modified Henderson and Pabis, Wang and Singh, logarithmic, two term, two term exponential, Midilli, approximation of diffusion and Verma *et al.*, model) were used for describing the drying behavior of sweet potato starches under tray, infrared and fluidized bed drying at 45, 55 and 65 °C. The results indicated that to reach a final moisture content of 10 % at 45, 55 and 65 °C, the drying time for tray drying was 15, 8.5 and 5.5 h for infrared drying was 12, 6.5 and 4.5 h and for fluidized bed drying was 0.42, 0.28 and 0.2 h respectively. The high R^2 (> 0.93), and low RMSE (0.002739 to 0.085240) and χ^2 (0.000003 to 0.007160) were found for all models, in which the Midilli model was found to be the best for explaining the starch drying behavior for all drying conditions. The generalized Midilli model also was developed for each drying method. The effective diffusivity (D_{eff}) for fluidized bed drying at 45 to 65 °C was 4.92×10^{-7} - 7.26×10^{-7} (m^2/s), significant higher than those in tray and infrared drying, ranging from 2.049×10^{-9} to 5.674×10^{-9} (m^2/s). The activation energies (E_a) in tray and infrared drying were 35.88 and 33.21 (kJ/mol) respectively, and nearly double that in fluidized bed drying (17.33 kJ/mol). The drying conditions only slightly affect the color, gel texture, swelling power, solubility and pasting properties of starches.

Keywords: Sweet potato starch, drying method, effective diffusivity, activation energy.

Introduction

Sweet potato (*Ipomoea batatas*), or kumara, a dicotyledonous plant that belongs to the family *Convolvulaceae*, is one of the most produced food crops in the world, especially in developing countries which produce more than 80 % of the total world production quantity. Due to easy growth and high productivity, it is considered as a traditional food crop and cultivated throughout in many Asian countries. Sweet potatoes are rich in starch (6.9 - 30.7 %, wb) in which amylose content ranges from 8.5 to 38 %, depending on the variety [1-3]. Therefore, it is considered as a good material for manufacturing starch and starch-based products. However, due to its limited application in food industries, the profits obtained from sweet

potato cultivation are much lower than those achieved from the other tuber crops. To raise the economic value of sweet potato roots, the production of highly value products from sweet potatoes needs to be studied. Sweet potato starch is one of those products because it can be used as a main ingredient, partially or totally substituted component for the other high price starches in many food processing industries.

During the process of starch extraction from tuber roots, particularly from sweet potato, three main steps which affect starch yield and properties are extraction, purification and drying. Most research relates to the extraction and purification [3-5], and only a few reports on the effects of

various drying conditions on starch [6] or flour properties [7,8] have been carried out to optimize starch or flour production conditions. Actually, the various types of drying methods can be used in starch or flour production such as tray drying, flash drying, drum drying, fluidized bed drying, and microwave-vacuum or infrared (IR) drying in which the heat can be added from outside objects by conduction, convection and radiation or generated within solid objects by electric resistance [9]. Among these methods, tray drying is favored due of its cheap cost and relatively ease of operation and control. But this method also poses many drawbacks such as lengthy drying time, high energy consumption and low drying efficiency because of rapid evaporation of surface moisture leading to surface hardness resulting in reduction of heat and moisture transfer and degradation of some quality attributes [10]. As infrared radiation is used to dry moist materials, the IR energy is transferred from the heating element to the product surface without heating the surrounding medium. The radiation impinges the exposed material, penetrates it and the energy of radiation converts into heat. The temperature gradient in the material reduces within a short period due to its intense heating. Therefore, under similar conditions, the infrared drying offers many advantages over tray drying, consisting of high drying rate, high energy efficiency, high quality finished products, uniform temperature in the product during the drying process, and a reduced necessity for air flow across the product [11,12]. Fluidized bed drying is renowned as the most efficient drying technology for particle materials because of its characteristic thorough mixing, which fosters vigorous heat and mass transfer, resulted in very short drying time [13].

In the drying process, the kinetics mainly depend on the operating conditions, material characteristics and equipment's design. Process modeling is one of the most important aspects to study drying behaviors of products and to design dryers effectively. The thin-layer drying models, describing the drying characteristics of agricultural materials, can be categorized as theoretical, semi-theoretical and empirical [14,15]. The theoretical models are based on the theory of moisture diffusion as liquid or vapor, represented by Fick's second law which has been applied for several materials that have no or a small volume reduction during drying. The Fick's model is also not

appropriate for materials which have high initial moisture content and present a long constant drying rate. Moreover, simplified assumptions such as constant diffusivity and a one-dimensional liquid diffusion theoretical model sometimes result in inadequate prediction to the moisture distribution. The empirical models are derived from statistical relationships and they directly correlate moisture content with time, having no physical fundamentals and therefore are unable to identify the prevailing mass transfer mechanism. In addition these types of models are only valid in the specific operational ranges for which they are developed. Although the semi-theoretical models may not able to explain the exact mechanism of moisture transport, they offer a compromise between theory and are easy to use and often give good estimation by incorporating lump values of other effects into the model parameters. In most work on drying, the semi-empirical thin-layer equations including the Newton model, Page model, the Henderson and Pabis model, the logarithmic model, the two-term model, the two-term exponential, the diffusion approach model, the Midilli model, the Verma *et al.* model, and the modified Henderson and Pabis model have been used to describe drying kinetics. These equations are useful for quick drying time estimations [16,17].

Besides modeling the drying process, the effects of drying conditions (temperature, RH, air velocity, etc.) on product quality need to be understood to obtain the desired quality products. For tray drying, various models that describe the drying behavior of different materials have been proposed by many authors for red pepper [18], eggplant [19], stanley plums [14], pistachio nuts [20], water chestnut (*Trapa natans*) [21] and potato slices [22]. For infrared drying, drying modeling has also been performed on various products such as rough rice [23], onion [11] and shrimp [24]. For fluidized bed drying, many researchers also focused on drying kinetics and modeling for various products such as chillies [25] and chopped coconut [26]. However, almost no literature mentions the drying kinetics of sweet potato starch using various drying methods.

The objectives of this study were to examine the drying behavior of tray, infrared and fluidized bed drying methods at 45, 55 and 65 °C on sweet potato starch, to develop a generalized model for

each drying method, to calculate effective diffusivity and activation energy, and to evaluate these drying conditions on starch properties in terms of color, gel texture, swelling power, solubility and pasting properties.

Materials and methods

Sample preparation

The white skin and yellow-red flesh color (*Kratai cultivar*) sweet potato variety was purchased from wholesalers, Thailand. The sweet potato roots were washed thoroughly, peeled, cut into small pieces which were then soaked in 0.2 % sodium metabisulfite with ratio of 1:2 for 15 min and ground in a blender for 5 min. The slurry was filtrated through a fabric filter to remove fibers and other components before passing through a 100-mesh sieve. The filtrate was allowed to stand undisturbed for 3 h. The collected starch was re-suspended in tap water, allowed to settle and water removed. This process was repeated three times to remove any pigment and sodium metabisulfite residues. The obtained starch was left to stand for 30 min at room temperature to remove surface water and then passed through a 1.6 mm-diameter sieve to create uniform size particles before drying.

Experimental apparatus

The isolated starches were dried under three drying methods namely, tray, infrared and fluidized bed drying at the same temperature 45, 55 and 65 °C for all methods.

Tray and infrared drying

About 280 g of starch was spread into a 1-cm layer on a metal tray whose dimensions were 25×15×1.5 cm (L×W×H). The drying air velocity was also fixed to be 1.2 m/s which was measured by an anemometer (Lutron, AM-4201, Taiwan). The dryers were operated for 1 h to achieve a steady state before running with the sample. The reduced sample weight was recorded at 1 min intervals for the first 20 min, and then increased to 10 min intervals during the drying process by the digital balance (NJW-3000, Japan). The drying process was carried out until a constant sample weight was obtained. The laboratory scale of tray and infrared dryers were developed by the Food Engineering and Bioprocess Technology workshop, Asian Institute of Technology.

The tray dryer consisted of the drying chamber constructed by stainless steel sheets as a rectangular tunnel. The temperature in the drying chamber was adjusted by the heater power control. The air velocity was controlled by adjusting openings at the end of the drying chamber. The heating system consisted of an 3,000 W electric heater placed inside a duct which was used to heat the air to the desired drying temperature. The airflow was passed over the sample layer during the drying process (**Figure 1**).

The basic design of the infrared dryer consisted of a stainless steel drying chamber and a 1,000 W ceramic infrared heater was installed at the top of the drying chamber (**Figure 2**).

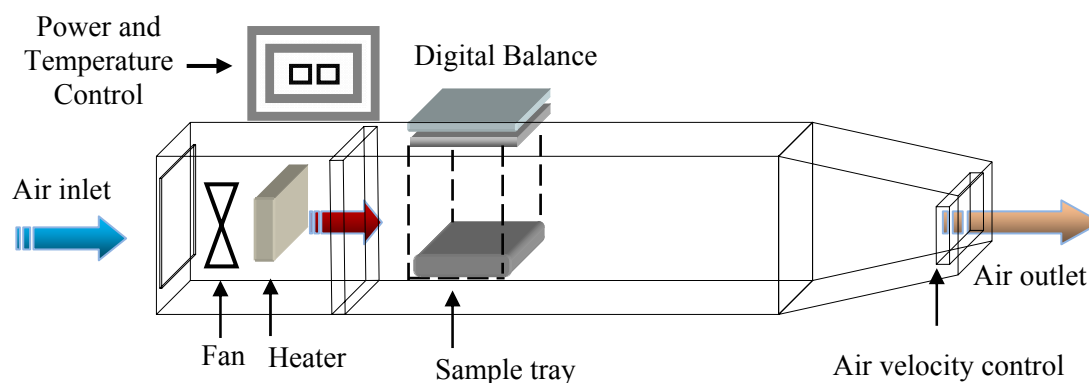


Figure 1 Tray dryer equipment.

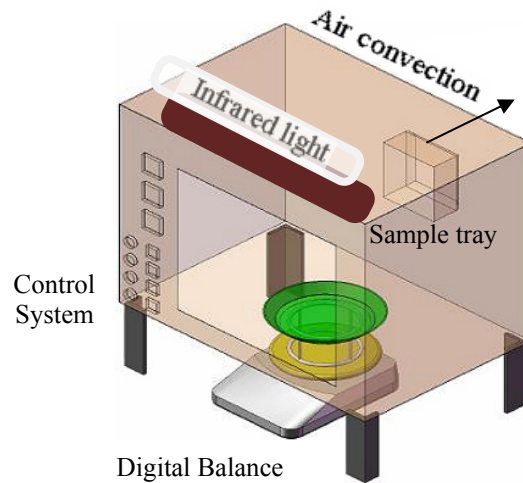


Figure 2 Infrared drying equipment.

Fluidized bed drying

The fluidized bed drier (Model F10A, Sherwood Scientific Ltd., UK) as shown in **Figure 3** was used for this experiment. The fluidized bed drier was operated for 30 min to achieve setting conditions before adding 280 g of the sample. The flow rate of hot air was also fixed at 1.2 m/s. The weight loss was recorded at 1 min interval during the drying process by using a digital balance (Sartorius, LC 62008, sensitivity 0.01 g).



Figure 3 Fluidized bed drying equipment.

Modeling of drying process

The initial moisture content (M_i) was determined according to the AACC [27] method. The equilibrium moisture content (M_e) of the sweet potato starch at various drying conditions was determined by following a dynamic method. The moisture content at which the sample weight was unchanged with drying time was the equilibrium moisture content [20]. These values, together with moisture content at interval drying time (M) were used to calculate the moisture ratio (MR) (Eq. 1) which was subsequently regressed with 11 mathematical models (**Table 1**).

$$MR = \frac{M - M_e}{M_i - M_e} \quad (1)$$

Table 1 The models used for modeling drying process [14].

No.	Model	Analytical expression ⁽¹⁾
1	Lewis	$MR = \exp(-k \times t)$
2	Page	$MR = \exp(-k \times t^n)$
3	Henderson and Pabis	$MR = a \times \exp(-k \times t)$
4	Wang and Singh	$MR = 1 + a \times t + b \times t^2$
5	Logarithmic	$MR = a \times \exp(-k \times t) + c$
6	Two term	$MR = a \times \exp(-k_1 \times t) + b \times \exp(-k_2 \times t)$
7	Two term exponential	$MR = a \times \exp(-k \times t) + (1-a) \times \exp(-k \times a \times t)$
8	Modified Henderson and Pabis	$MR = a \times \exp(-k \times t) + b \times \exp(-g \times t) + c \times \exp(-h \times t)$
9	Midilli	$MR = a \times \exp(-k \times t^n) + b \times t$
10	Approximation of diffusion	$MR = a \times \exp(-k \times t) + (1-a) \times \exp(-k \times b \times t)$
11	Verma <i>et al.</i>	$MR = a \times \exp(-k \times t) + (1-a) \times \exp(-g \times t)$

⁽¹⁾ Where $MR = (M - M_e)/(M_o - M_e)$, moisture ratio (dimensionless); a, b, c, g, h, k, k₁, k₂ and n = drying constants; t = drying time (h).

There were some criteria to select the best model to describe the drying curve, namely correlation coefficient (R^2), reduced chi-square (χ^2) which was the mean square of the deviations between the experimental and calculated values for the models and Root Mean Square Error analysis (RMSE) that was the deviation between the predicted and experimental values [18]. The model to be selected must show the highest value of R^2 , the lowest values RMSE and chi-square (χ^2) and ease of use in practice.

$$RMSE = \left[\frac{1}{N} \sum_{i=1}^N (MR_{pre,i} - MR_{exp,i})^2 \right]^{1/2} \quad (2)$$

$$\chi^2 = \frac{\sum_{i=1}^n (MR_{exp,i} - MR_{pre,i})^2}{N - n} \quad (3)$$

Where $MR_{exp,i}$ = the i^{th} experimentally observed moisture ratio
 $MR_{pre,i}$ = the i^{th} predicted moisture ratio
 n = number of constants
 N = number of observations

By using regression analysis between the drying constant and coefficient values of the best model and drying temperature, a generalized equation was proposed for estimation of the moisture ratio as well as moisture content of the sample at any time during the drying process within the considered temperature range for each drying method.

Determination of moisture diffusivity and activation energy

The Fick's second law of diffusion is a mathematic equation which is commonly used for describing the drying process and is based on the assumptions: moisture migration is only by diffusion; there is uniform initial moisture distribution; the effective moisture diffusivity and temperature are constant; and sample shrinkage is negligible [28].

$$\frac{dM}{dt} = D_{eff} \frac{d^2M}{dr^2} \quad (4)$$

Where M = the local moisture content (kg water/kg dry solids)

r = the diffusion path (m)
 t = the time (s)
 D_{eff} = the effective moisture diffusivity (m^2/s)

Crank [29] solved the Fick's second law of diffusion for an infinitive slab (Eq. 5) and for a spherical object (Eq. 6) of unsteady state diffusion used to determine the moisture ratio. The initial

and boundary conditions are that firstly the moisture is initially distributed uniformly throughout the sample, secondly the mass transfer is symmetric with respect to the centre of the particle layer, thirdly the surface moisture content of the samples instantaneously reaches equilibrium with the conditions of the surrounding air.

$$\text{For infinitive slab: } MR = \frac{8}{\pi^2} \sum_{n=0}^{\infty} \frac{1}{(2n+1)} \exp\left(-\frac{(2n+1)^2 \pi^2 D_{\text{eff}} t}{4L^2}\right) \quad (5)$$

$$\text{For spherical particles: } MR = \frac{6}{\pi^2} \sum_{n=0}^{\infty} \frac{1}{n^2} \exp\left(-n^2 \pi^2 \frac{D_{\text{eff}} t}{R^2}\right) \quad (6)$$

Where R = the radius of particle (m)
 L = the thickness of slab (m)

For tray and infared drying because the sample was spread into a 1 cm layer on a metal tray, it could be considered to be an infinitive slab while for fluidized bed drying the sample was subjected to hot air flow in forms of separated particles, the Fick's second law of diffusion for a spherical object therefore was used to find effective diffusivity and activation of energy. For

long drying periods ($MR < 0.6$), these equations can be simplified to the first term ($n = 0$ in Eq. 5 and $n = 1$ in Eq. 6) of the series with small errors and taking the natural logarithm of both members results in the following equation (Eq. 7 and Eq. 8). The effective diffusivity was determined from the slope obtained by plotting $\ln(MR)$ versus drying time (t).

$$\text{For infinitive slab: } \ln(MR) = \ln\left(\frac{8}{\pi^2}\right) - \frac{\pi^2 D_{\text{eff}} t}{4L^2} \quad (7)$$

$$\text{For spherical particles: } \ln(MR) = \ln\left(\frac{6}{\pi^2}\right) - \frac{\pi^2 D_{\text{eff}} t}{R^2} \quad (8)$$

The energy of activation was calculated from an Arrhenius equation (Eq. 9) by taking the natural

logarithm and plotting a graph between $\ln(D_{\text{eff}})$ versus $(1/T)$ (Eq. 10).

$$D_{\text{eff}} = D_o \exp\left(-\frac{E_a}{RT}\right) \quad (9) \quad \rightarrow \quad \ln(D_{\text{eff}}) = \ln(D_o) - \frac{E_a}{RT} \quad (10)$$

Where D_o = the pre-exponential factor of the Arrhenius equation (m^2/s)
 E_a = the activation energy of the moisture diffusion (kJ/mol)
 T = the air absolute temperature (K)
 R = the gas constant (8.3143 kJ/kmol.K)

Determination of starch properties

Swelling power and solubility of starch was determined by the method introduced by Shimelis *et al* [30]. Gel texture was determined by using Instron TA.XT2 Plus, uniaxial compression (Stable Micro System, USA) as reported by Pons *et al.* [31]. The starch pasting properties in terms of pasting temperature (P_{temp}), peak viscosity (PV), trough viscosity (TV), breakdown (BD = PV-TV), final viscosity (FV) and setback viscosity SB = FV-TV) was determined by Rapid Visco Analyzer (Newport Scientific, Australia) (AACC) [27]. The color values of starches in terms of L* (lightness to darkness), a* (redness to greenness) and b* (yellowness to blueness) values were measured with a Hunterlab Colorimeter (Colorflex, USA), the whiteness value was obtained using the following equation.

$$\text{Whiteness} = 100 - \left[(100 - L)^2 + a^2 + b^2 \right]^{1/2} \quad (11)$$

Data analysis

Microsoft Excel 2007 and MATLAB 7.0 version were used to analyze all drying data. All experiments and analysis were performed in three replications. The data were subjected to statistical one-way ANOVA, Fisher's Least Significant Difference (LSD) or Duncan Multiple Range Tests (DMRT) to compare among treatments at the 5 % significance level by using SPSS version 16.

Results and discussion

Equilibrium moisture content (EMC)

The EMC at various drying temperatures in both tray and fluidized bed drying methods was similar, but slightly lower than those in infraed drying (**Table 2**). This could be because the heat was transferred from the heat source to the product by radiation without heating air as a medium in infrared drying, resulting in higher air relative humidity and EMC [11,12]. The EMC reduced with increasing drying temperature due to a decrease in the relative air humidity at higher temperature.

Table 2 Equilibrium moisture content (EMC) at different drying conditions.

Drying method	Drying temperature (°C)	EMC, % db ⁽¹⁾
Tray drying	45	7.59 ± 0.10
	55	4.52 ± 0.14
	65	2.29 ± 0.30
Infrared drying	45	8.11 ± 0.18
	55	5.19 ± 0.46
	65	3.77 ± 0.50
Fluidized bed drying	45	7.65 ± 0.41
	55	4.55 ± 0.10
	65	2.76 ± 0.18

⁽¹⁾All values are means of three determinations. Values are means ± standard deviation.

Drying characteristics

For the tray and infrared drying (**Figure 4**), after undergoing a short heating period during which the drying rate significantly increased, the drying process occurred only in the falling-rate drying period, there was almost no constant-rate drying period. This indicated that the mechanism of mass transfer in the material was a moisture diffusion process [14]. During the falling-rate period, the initial drying rate was high as moisture for evaporation came from regions near the surface. As drying progressed, the drying rate gradually decreased as water to be evaporated must be transported from inner layers to the surface. Therefore, the falling rate region expressed an increase in resistance to heat and mass transfer inside the material [20]. Moreover, the rapid evaporation of surface moisture could lead to formation of a surface hard layer which inhibited the moisture removal from material, thus reducing the drying rate. At the same temperature, the drying rate of infrared drying was higher than that of tray drying, resulting in a shorter drying time. In tray drying, it took about 15, 8.5 and 5.5 h to get about 10 % (wb) moisture content at 45, 55 and 65 °C respectively. To obtain the desired moisture content, the drying time for infrared drying was 12, 6.5 and 4.5 h at 45, 55 and 65 °C respectively (**Figure 5**). The shorter drying time in infrared drying compared to tray drying could be explained by the penetration of radiation into the material offered more uniform heating, reduced moisture gradient during heating as well as drying period [12] or caused water molecules to vibrate, at that state less energy was needed to transport them out of the porous products [32]. The shortness of drying time in infrared drying compared to tray drying which was observed in

this research was similar to the results reported on onion slices [11] and shrimp [24].

The constant-rate period occurred in a very short time in comparison with the whole drying time and could be neglected in the tray and infrared drying. While in fluidized bed drying there were three obvious drying periods and the drying process almost happened in constant and falling rate periods (**Figure 4**). In fluidized bed drying, because of thorough mixing, all small particles were exposed simultaneously to hot air, and the heat and mass transfer occurred very fast, resulting in almost no surface hardness which hinders moisture removal in tray and infrared drying, thus significantly higher drying rates and shorter drying times were observed compared to other methods in this research [23]. It required only 0.42, 0.28 and 0.2 h to obtain the desired moisture content at 45, 55 and 65 °C respectively (**Figure 5**). As with other drying methods, the drying time was markedly reduced as the drying temperature increased. The drying curve at higher temperature was steeper than that at lower temperature (**Figure 6**). The drying time reduced nearly 2 to 3 times as the drying temperature increased from 45 to 65 °C in all drying methods. The increase in drying temperature was responsible for increasing the heating rate and water vapor pressure inside the material, thus accelerating the water migration inside the product, consequently leading to higher drying rates and shorter drying times [11]. The effects of drying temperature on drying rate in tray, infrared and fluidized bed drying were also well explained by Akpınar *et al.* [18], Tasirin *et al.* [25], Tirawanichakul *et al.* [24] and Madhiyanon *et al.* [26].

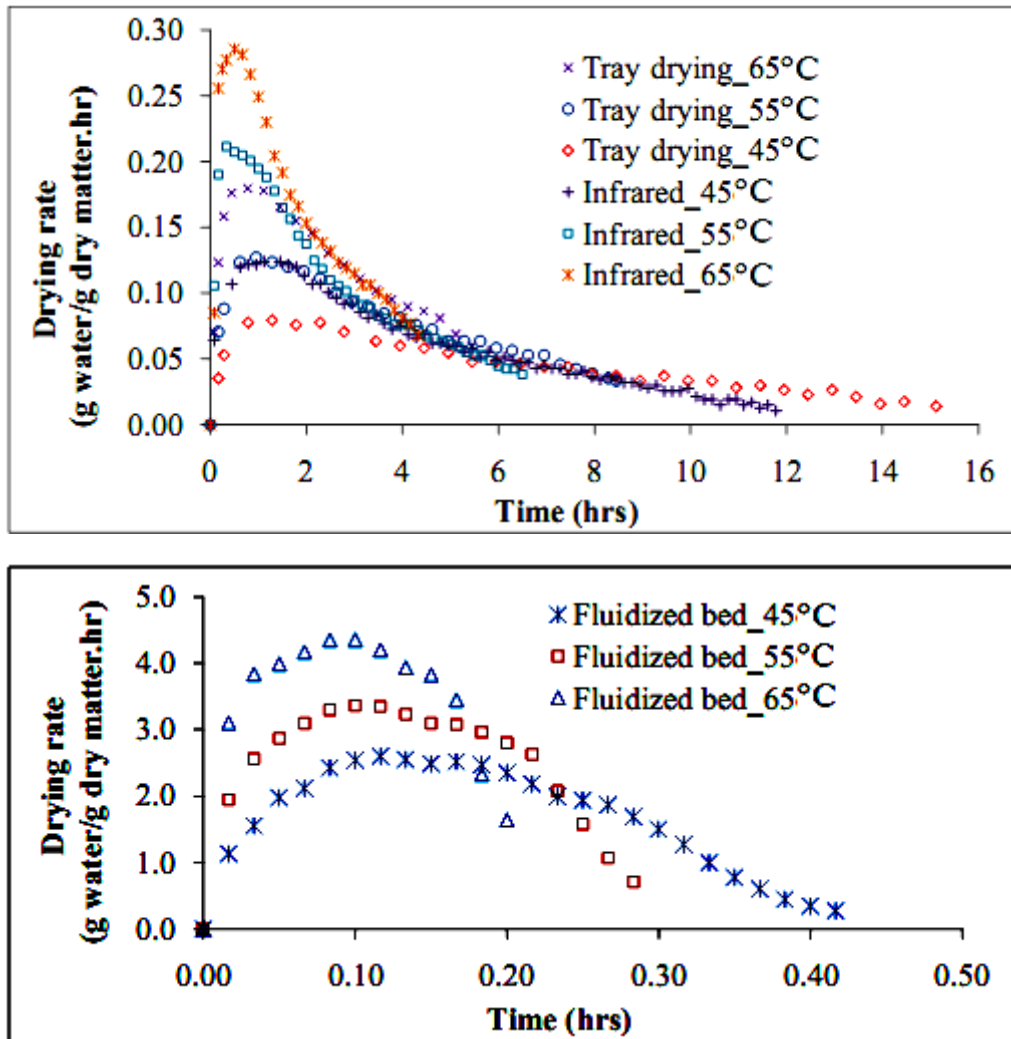


Figure 4 The drying rate at different temperatures in tray, infrared and fluidized bed drying.

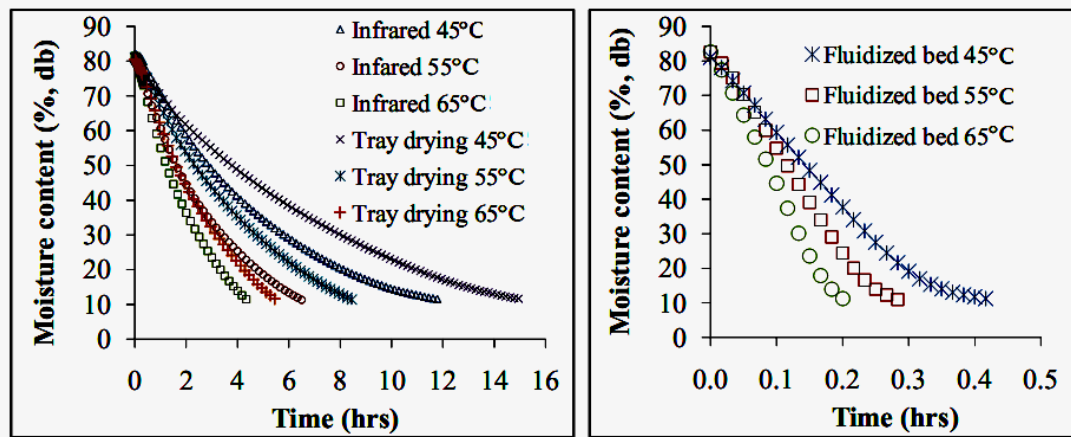


Figure 5 The changes in MC (% db) with drying time at different drying temperatures in tray, infrared and fluidized bed drying.

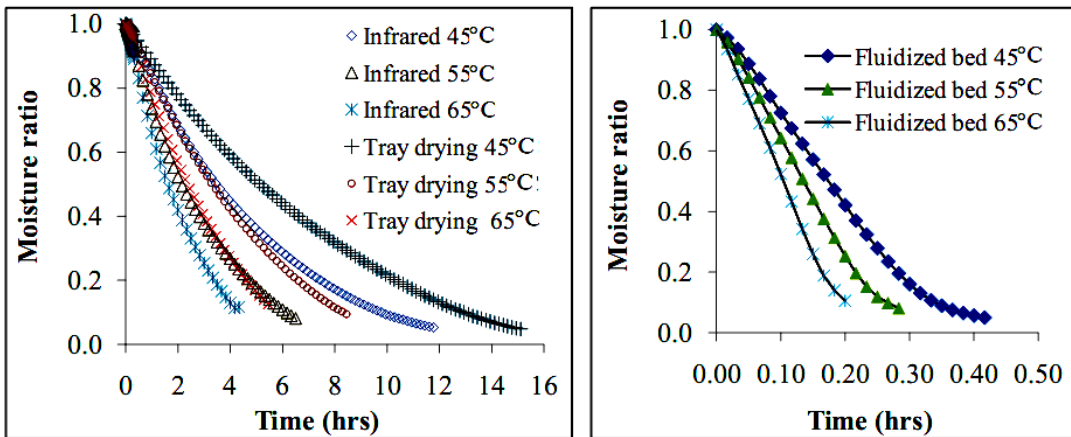


Figure 6 The changes in moisture ratio (MR) with drying time in tray, infrared and fluidized bed drying.

Development of drying modeling

The degree of fitness of 11 models was compared on the basis of R^2 , RMSE and χ^2 tests. The results from Tables 3 - 5 show that high R^2 (> 0.93) and low in RMSE (0.002739 to 0.085240) as well as χ^2 (0.000003 to 0.007160) were found for all drying models. This indicated that all models could be used for describing drying behavior of sweet potato starch. However, for each drying method, the highest R^2 values (0.9972 to 1.000), the lowest RMSE (0.001623 to 0.019190) and χ^2 (0.000003 to 0.000412) at all drying temperature was observed in Midilli model. This model could be shown as $MR = a \cdot \exp(-k \cdot t^n) + b \cdot t$ in which the drying constants a, k, n and b at different

drying air temperature are also expressed in Tables 3-5 for tray, infrared and fluidized drying method respectively. Interestingly, the Midilli model was also found as the best model to describe the drying behavior for plum [14], eggplant [19], potato, apple and pumpkin [15].

Because of high R^2 value ($R^2 > 0.93$), almost all drying constants and coefficients showed a good linear relationship to drying temperature, except to n value in infrared drying which had a good fit to a polygonal curve. By substituting the equations which expressed relationship between drying constants and coefficients and drying temperature into the Midilli model, a generalized Midilli model for each drying method can be expressed as follows.

- For tray drying

$$MR = (0.0001 \times T + 0.9995) \times \exp[-(0.006 \times T - 0.1700) \times t^{(0.005 \times T + 0.807)}] + (-0.00024 \times T + 0.00357) \times t \tag{11}$$

- For infrared drying

$$MR = (0.00015 + 0.99908) \times \exp[-(0.011 \times T - 0.314) \times t^{(0.00049 \times T^2 - 0.0536 \times T + 2.485)}] + (-0.0003 \times T + 0.01016) \times t \tag{12}$$

- For fluidized bed drying

$$MR = (0.00018 \times T + 0.9789) \times \exp[-(0.221 \times T + 1.078) \times t^{(-0.006 \times T + 1.890)}] + (-0.035 \times T + 1.571) \times t \tag{13}$$

Table 3 Statistical results of modeling criteria (R^2 , RMSE and χ^2), and drying constants and coefficients of tray drying.

Models	Drying temperature (°C)								
	45			55			65		
	R ²	RMSE	χ ²	R ²	RMSE	χ ²	R ²	RMSE	χ ²
Lewis (1)	0.9911	0.03105	0.00096	0.992	0.029	0.00082	0.991	0.03007	0.00090
Page (2)	0.9981	0.01446	0.00021	1.000	0.008	0.00006	1.000	0.00589	0.00004
Henderson and Pabis (3)	0.9928	0.02817	0.00079	0.995	0.024	0.00057	0.995	0.02333	0.00054
Wang and Singh (4)	0.9995	0.00777	0.00006	1.000	0.006	0.00004	0.999	0.00896	0.00008
Logarithmic (5)	0.9999	0.00255	0.00001	1.000	0.004	0.00002	1.000	0.00581	0.00003
Two term (6)	0.9983	0.01362	0.00019	0.999	0.013	0.00017	0.997	0.01731	0.00030
Two term exponential (7)	0.9981	0.01440	0.00021	0.999	0.008	0.00006	1.000	0.00685	0.00005
Modified Henderson and Pabis (8)	0.9985	0.01292	0.00017	0.995	0.023	0.00071	0.992	0.02996	0.00092
Midilli (9)	0.9999	0.00274	0.00001	1.000	0.002	0.00000	1.000	0.00236	0.00001
Approximation of diffusion (10)	0.9984	0.01338	0.00018	1.000	0.007	0.00005	1.000	0.00655	0.00004
Verma <i>et al</i> (11)	0.9984	0.01343	0.00018	1.000	0.007	0.00005	0.991	0.03071	0.00092

Models	Drying constants and coefficients								
	45			55			65		
1	k = 0.1473			k = 0.2234			k = 0.3097		
2	k = 0.1004, n = 1.193			k = 0.1658, n = 1.203			k = 0.2439, n = 1.224		
3	k = 0.1519, a = 1.028			k = 0.2316, a = 1.029			k = 0.3237, a = 1.032		
4	a = -0.113, b = 0.00336			a = -0.1764, b = 0.008285			a = -0.245, b = 0.01551		
5	k = 0.1040, a = 1.22, c = -0.2149			k = 0.1563, a = 1.26, c = -0.2477			k = 0.2048, a = 1.333, c = -0.3171		
6	a = 15.88, b = -14.88, k1 = 0.2386, k2 = 0.2477			a = 28.57, b = -27.56, k1 = 0.3402, k2 = 0.3458			a = 31.73, b = -30.71, k1 = 0.4411, k2 = 0.4462		
7	k = 0.2001, a = 1.721			k = 0.3130, a = 1.746			k = 0.4483, a = 1.777,		
8	k = 0.2410, a = 9.689, b = -8.716, c = 0.04248, g = 0.2583, h = 3.463			k = 0.2356, a = 0.9855, b = -0.04585, c = 0.08796, g = 0.1666, h = 0.2421			k = 0.1455, a = -11.92, b = 0.5282, c = 12.43, g = 0.486, h = 0.1486		
9	k = 0.1155, n = 1.029, a = 1.004, b = -0.007506			k = 0.1713, n = 1.096, a = 1.005, b = -0.008952			k = 0.2415, n = 1.13, a = 1.006, b = -0.01229		
10	k = 0.1155, a = -16.07, b = 0.9645			k = 0.4100, a = -5.702, b = 0.9034			k = 0.5841, a = -9.197, b = 0.9331		
11	k = 0.2503, a = -14.31, g = 0.2405			k = 0.4133, a = -5.004, g = 0.3685			k = 0.309, a = 1.127, g = 0.3042		

Table 4 Statistical results of modeling criteria (R^2 , RMSE and χ^2), and drying constants and coefficients of infrared drying.

Models	Drying temperature (°C)								
	45			55			65		
	R^2	RMSE	χ^2	R^2	RMSE	χ^2	R^2	RMSE	χ^2
Lewis (1)	0.9963	0.02083	0.00043	0.998	0.01533	0.00024	0.995	0.02225	0.00049
Page (2)	0.9997	0.00646	0.00004	1.000	0.00664	0.00004	1.000	0.00630	0.00004
Henderson and Pabis (3)	0.9976	0.01690	0.00029	0.999	0.01178	0.00014	0.998	0.01465	0.00021
Wang and Singh (4)	0.9986	0.01272	0.00016	0.999	0.01261	0.00016	0.999	0.00977	0.00010
Logarithmic (5)	0.9998	0.00487	0.00002	1.000	0.00469	0.00002	1.000	0.00601	0.00004
Two term (6)	0.9987	0.01249	0.00016	0.999	0.00881	0.00008	0.999	0.01220	0.00015
Two term exponential (7)	0.9996	0.00684	0.00005	1.000	0.00710	0.00005	1.000	0.00766	0.00006
Modified Henderson and Pabis (8)	0.999	0.01108	0.00009	0.999	0.01220	0.00015	0.998	0.01436	0.00021
Midilli (9)	0.9999	0.00335	0.00001	1.000	0.00444	0.00002	1.000	0.00484	0.00002
Approximation of diffusion (10)	0.9996	0.00722	0.00005	1.000	0.00709	0.00005	0.999	0.01090	0.00012
Verma <i>et al</i> (11)	0.9989	0.01157	0.00013	1.000	0.00709	0.00005	0.998	0.01437	0.00021

Models	Drying constants and coefficients		
	45	55	65
1	k = 0.2093	k = 0.3310	k = 0.4427
2	k = 0.1675, n = 1.134	k = 0.2993, n = 1.090	k = 0.4002, n = 1.139
3	k = 0.2151, a = 1.025	k = 0.3386, a = 1.017	k = 0.4615, a = 1.028
4	a = -0.1632, b = 0.007225	a = -0.2683, b = 0.02022	a = -0.3611, b = 0.03637
5	k = 0.1788, a = 1.103, c = -0.08937	k = 0.2896, a = 1.089, c = -0.07983	k = 0.3665, a = 1.147, c = -0.1303
6	a = 23.42, b = -22.4, k1 = 0.2714, k2 = 0.2746	a = 7.297, b = -6.285, k1 = 0.4205, k2 = 0.4367	a = -7.977, b = 9.003, k1 = 0.351, k2 = 0.3622
7	k = 0.2716, a = 1.648	k = 0.4157, a = 1.578	k = 0.5977, a = 1.6770
8	k = 0.1296, a = -13.74, b = 14.63, c = 0.1378, g = 0.1335, h = 0.2726	k = 0.3379, a = 0.1123, b = -0.01885, c = 0.9239, g = 0.2911, h = 0.3377	k = 0.2048, a = -11.22, b = 0.4814, c = 11.77, g = 0.6216, h = 0.211
9	k = 0.1779, n = 1.065, a = 1.006, b = -0.003092	k = 0.3042, n = 1.019, a = 1.007, b = -0.006748	k = 0.3990, n = 1.071, a = 1.009, b = -0.009079
10	k = 0.1255, a = 4.67, b = 0.8669	k = 0.5334, a = -2.463, b = 0.8629	k = 0.2364, a = 4.577, b = 0.8208
11	k = 0.2934, a = -30.83, g = 0.29	k = 0.5183, a = -3.713, g = 0.4679	k = 0.2800, a = 11.19, g = 0.2669

Table 5 Statistical results of modeling criteria (R^2 , RMSE and χ^2), and drying constants and coefficients of fluidized bed drying.

Models	Drying temperature (°C)								
	45			55			65		
	R^2	RMSE	χ^2	R^2	RMSE	χ^2	R^2	RMSE	χ^2
Lewis (1)	0.9374	0.08127	0.00659	0.933	0.08166	0.00658	0.937	0.07737	0.00591
Page (2)	0.9978	0.01568	0.00020	0.997	0.01890	0.00026	0.994	0.02636	0.00045
Henderson and Pabis (3)	0.9607	0.06575	0.00434	0.955	0.06885	0.00472	0.951	0.07302	0.00489
Wang and Singh (4)	0.9897	0.03360	0.00107	0.992	0.02866	0.00075	0.994	0.02501	0.00064
Logarithmic (5)	0.9924	0.02956	0.00007	0.994	0.02541	0.00058	0.995	0.02421	0.00064
Two term (6)	0.9889	0.03654	0.00125	0.984	0.04451	0.00194	0.990	0.03722	0.00118
Two term exponential (7)	0.9922	0.02929	0.00081	0.990	0.03197	0.00092	0.987	0.03831	0.00125
Modified Henderson and Pabis (8)	0.9925	0.03155	0.00094	0.986	0.04457	0.00023	0.992	0.03711	0.00106
Midilli (9)	0.9986	0.01308	0.00011	0.998	0.01454	0.00011	0.997	0.01919	0.00041
Approximation of diffusion (10)	0.9682	0.06040	0.00362	0.936	0.08524	0.00716	0.958	0.07091	0.00476
Verma <i>et al</i> (11)	0.9886	0.03622	0.00124	0.989	0.03586	0.00120	0.991	0.03333	0.00113

Models	Drying constants and coefficients		
	45	55	65
1	k = 4.7700	k = 5.9600	k = 7.6830
2	k = 12.1600, n = 1.608	k = 18.7800, n = 1.623	k = 26.7600, n = 1.582
3	k = 5.4440, a = 1.135	k = 6.7630, a = 1.118	k = 8.8970, a = 1.1
4	a = -3.318, b = 2.177	a = -3.932, b = 1.762	a = -5.116, b = 1.742
5	k = 2.3700, a = 1.696, c = -0.6359	k = 1.7630, a = 2.559, c = -1.52	k = 1.4020, a = 3.98, c = -2.957
6	a = -29.29, b = 30.31, k1 = 0.6617, k2 = 0.748	a = -26.46, b = 27.44, k1 = -0.4765, k2 = -0.3457	a = -11.35, b = 12.34, k1 = -0.8073, k2 = -0.3972
7	k = 7.809, a = 2.0490	k = 9.952, a = 2.0400	k = 13.23, a = 2.0180
8	k = 2.2660, a = 2.047, b = -0.9754, c = -0.005345, g = 0.5094, h = 0.6782	k = -8.5380, a = 0.04976, b = 6.437, c = -5.459, g = -0.2082, h = -1.039	k = -2.6760, a = -11.98, b = 1.461, c = 11.52, g = 2.12, h = -2.642
9	k = 10.76, n = 1.582, a = 0.987, b = -0.08216	k = 13.76, n = 1.544, a = 0.9888, b = -0.2729	k = 15.1800, n = 1.449, a = 0.9906, b = -0.7929
10	k = 2.2970, a = -37.32, b = 1.022	k = 5.0120, a = -7.008, b = 1.024	k = 4.0330, a = -19.71, b = 1.039
11	k = 1.1230, a = 5.974, g = 0.6747	k = 1.2450, a = 17.68, g = 1.057	k = 1.3750, a = 17.73, g = 1.114

There was good agreement between the predicted moisture ratio obtained from the above general Midilli models (Eq. 11, 12 and 13) and experimental values for all drying conditions as shown in **Figure 7** ($R^2 > 0.98$). This meant that those general models were applicable for describing the drying behavior of sweet potato starch at drying air temperatures of 45 to 65 °C in tray, infrared and fluidized bed drying.

Determination of effective diffusivity (D_{eff}) and energy of activation (E_a)

Among the three drying methods the D_{eff} in fluidized bed drying was the highest, following by infrared drying (**Table 6**). The higher D_{eff} indicates

the water molecules were removed from the material more rapidly and also shorter drying time. That explained why the drying rate in fluidized bed drying is significantly higher than that in the remaining drying methods. For the same drying method, D_{eff} increased with increasing drying air temperature because of an acceleration of mass transfer at elevated temperature. It is clear that D_{eff} depends on drying temperature [33]. These calculated values which range from 2.049×10^{-9} to 4.92×10^{-7} (m^2/s) depending on the drying conditions were in the general range for food materials which is 10^{-13} to 10^{-6} m^2/s [34].

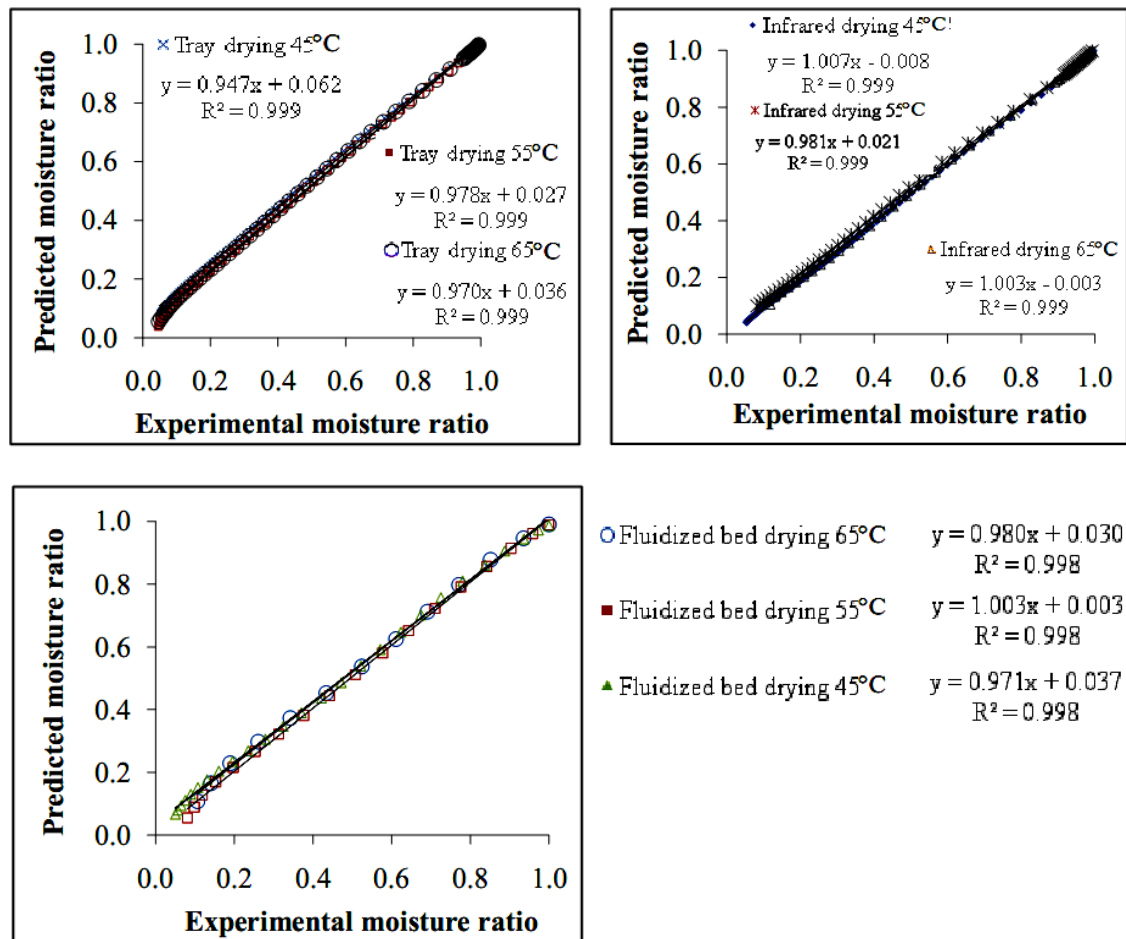


Figure 7 Comparison of experimental and predicted MR by the generalized Midilli model (Eq. 11, 12 and 13) for tray, infrared and fluidized bed drying respectively.

Table 6 The effective diffusivity (m^2/s) in tray, infrared and fluidized bed drying.

Temperature ($^{\circ}C$)	Drying methods		
	Tray	Infrared	Fluidized bed
45	2.049×10^{-9}	2.702×10^{-9}	4.92×10^{-7}
55	3.242×10^{-9}	4.278×10^{-9}	5.89×10^{-7}
65	4.571×10^{-9}	5.674×10^{-9}	7.26×10^{-7}

Table 7 The Arrhenius constant and activation energy in different drying methods.

Drying method	Arrhenius constant, D_0 (m^2/s)	Activation energy, E_a (kJ/mol)
Tray drying	16.37×10^{-4}	35.88
Infrared drying	7.94×10^{-4}	33.21
Fluidized bed drying	1.00×10^{-7}	17.33

The activation energy is the minimum energy required or the energy which must be overcome in order for moisture diffusion to occur inside the material. The E_a in tray and infrared drying were 35.88 and 33.21 kJ/mol respectively, nearly double the value of that in fluidized bed drying which was about 17.33 kJ/mol (**Table 7**). This indicated markedly higher drying rates in fluidized bed drying compared to tray and infrared drying. This finding was similar to research results on onion slices [32] in which the smaller E_a , the higher the drying rate which was found. These E_a values were in good agreement with data reported by various authors such as 30.79 kJ/mol for pistachio nuts [20], 39.49 - 42.34 kJ/mol for potato slices [22], 25.94 kJ/mol for chopped coconut [26]. As the drying temperature increased, the energy barrier for activating moisture diffusion is relatively easier to overcome, leading to higher drying rates, however there is a compromise between the drying rate and the final product quality [20].

Effect of drying conditions on the sweet potato starch properties

At the same drying temperature, the starches obtained from fluidized bed and infrared drying

seem to show more lightness (L^*) and whiteness, less yellowness (b^*) and greenness (a^*) than those achieved by tray drying (**Table 8**) because of the longer drying time in tray drying compared to the others resulting in degradation of starch color. The better product quality in fluidized bed and infrared drying compared to tray drying or sun drying was also reported by Tasirin *et al.* [25] on chilies, Shi *et al.* [35] on blueberries and Tirawanichakul *et al.* [24] on shrimp. In the tray and infrared drying methods, starches which were dried at 55 $^{\circ}C$ gave better quality in terms of lightness, whiteness, yellowness and greenness compared to starch treated at 45 and 65 $^{\circ}C$. This was because of the longer drying time at 45 $^{\circ}C$ and high drying temperature at 65 $^{\circ}C$ caused unwanted starch color changes. While in the fluidized bed drying, due to the very short drying time, the starch color in term of greenness (a^*) and yellowness (b^*) was not different at the three drying temperatures, but starch dried at 65 $^{\circ}C$ was slight darker than starches dried at 45 and 55 $^{\circ}C$. These changes in starch color might be because of oxidation or isomerization of remaining pigments in starches under heating [8].

Table 8 The color of sweet potato starches at various drying conditions.

Drying conditions	L*	a*	b*	Whiteness
Tray_45 °C	92.45 ^c ± 0.28	-1.31 ^{cd} ± 0.05	5.97 ^d ± 0.08	90.29 ^h ± 0.18
Tray_55 °C	93.45 ^d ± 0.26	-1.22 ^e ± 0.03	4.96 ^{bc} ± 0.10	91.69 ^e ± 0.15
Tray_65 °C	93.35 ^d ± 0.17	-1.25 ^{de} ± 0.05	5.27 ^c ± 0.23	91.42 ^f ± 0.14
Infrared_45 °C	94.29 ^{bc} ± 0.27	-1.63 ^a ± 0.04	4.99 ^{bc} ± 0.28	92.24 ^d ± 0.06
Infrared_55 °C	94.88 ^a ± 0.26	-1.54 ^b ± 0.06	4.77 ^b ± 0.12	92.83 ^b ± 0.14
Infrared_65 °C	93.44 ^d ± 0.19	-1.54 ^b ± 0.04	5.83 ^d ± 0.12	91.09 ^g ± 0.13
Fluidized_45 °C	94.60 ^{ab} ± 0.21	-1.36 ^c ± 0.04	3.98 ^a ± 0.21	93.15 ^a ± 0.05
Fluidized_55 °C	94.48 ^{ab} ± 0.31	-1.31 ^{cd} ± 0.04	4.12 ^a ± 0.22	92.98 ^{ab} ± 0.12
Fluidized_65 °C	93.97 ^c ± 0.14	-1.30 ^{cd} ± 0.02	4.24 ^a ± 0.21	92.51 ^c ± 0.03

(*) All values are mean of three replications. L* : lightness/darkness value (+ = lightness, - = darkness), greenness (a value) and yellowness (b value). Values are means ± standard deviation. Within the same pattern column, the values with different letters are significantly difference at $p < 0.05$ by LSD test.

Similar to color, these drying conditions only slightly affected gel texture, swelling power, solubility and pasting properties (Tables 9 - 10). For the pasting properties, it was found that the peak and trough viscosity were affected by drying temperature and method while the other pasting properties was almost unchanged. In general, the highest peak and trough viscosity were observed in fluidized bed drying, followed by those in infrared drying, increasing slightly with an increase in drying temperature. The results are consistent with the conclusion of Lai [36] in which the minimum moisture content and temperature needed to significantly change the pasting properties was 34.8 % (db) and 85 °C respectively. The gel texture in terms of hardness and stickiness was not affected by these drying conditions. The soluble amylose is considered primarily responsible for gel formation, but these drying conditions had almost no effect on starch granule or integrity, resulting in similar products to those in which amylose has leached from the starches dried under various conditions [37].

The solubility and swelling power of starches dried under these conditions were almost unchanged at about 13 and 21 % respectively. The swelling power and solubility were affected by amylose content, structural characteristics of

amylose and amylopectin, the presence of non-carbohydrate substances [1,3] The formation of an amylose-lipid complex during heating which restricted the swelling and solubility. The correlation between swelling power as well as solubility and gel texture has reported by Collado and Corke [38] who found that there was a negative correlation between starch solubility and firmness of starch gel texture, Lee *et al.* [39] claimed that surface stickiness of starch noodles exhibited positive correlation to solubility.

The drying at 45, 55 and 65 °C does not effect starch properties because the drying temperature is lower than the gelatinization temperature. These results were similar to the findings of Malumba *et al.* [40] on corn starch. The starches with 60 % moisture content would gelatinize at 70 °C [41] thus the properties of starch with 45 % of MC which was dried under various conditions as in this research were almost unchanged. Moreover, separation of other components out of starch before drying prevented the reaction and effects of those components on the starch which might result in changing of the starch properties.

Table 9 The gel texture, swelling power and solubility of sweet potato starches at various drying conditions.

Drying conditions	Hardness, (g-force)	Stickiness, (g-force)	Solubility, (%)	Swelling power, (%)
Tray_45 °C	245 ^a ±14	26 ^b ±01	12.98 ^a ±0.17	21.16 ^{ab} ±0.32
Tray_55 °C	244 ^a ±10	26 ^b ±1.4	13.13 ^a ±0.68	21.31 ^{ab} ±0.81
Tray_65 °C	238 ^a ±05	25 ^b ±0.9	13.47 ^a ±0.37	20.58 ^b ±0.99
Infrared_45 °C	235 ^a ±12	23 ^a ±1.4	13.04 ^a ±0.47	21.30 ^{ab} ±0.66
Infrared_55 °C	239 ^a ±03	24 ^b ±0.8	13.19 ^a ±0.44	21.77 ^{ab} ±0.61
Infrared_65 °C	240 ^a ±05	25 ^b ±1.1	13.40 ^a ±0.53	22.04 ^a ±0.48
Fluidized_45 °C	242 ^a ±01	25 ^b ±0.8	13.41 ^a ±0.43	21.21 ^{ab} ±0.83
Fluidized_55 °C	237 ^a ±06	24 ^a ±0.7	13.36 ^a ±0.53	21.49 ^{ab} ±0.65
Fluidized_65 °C	238 ^a ±03	25 ^b ±0.8	13.53 ^a ±0.42	22.13 ^a ±0.46

Notes: All values are mean of three replications. Values are means ± standard deviation. Within the same column, the values with different letters are significantly different at p < 0.05 by LSD test.

Table 10 The pasting properties of sweet potato starches at various drying conditions.

Drying conditions	Pasting properties						
	PV (RVU)	TV (RVU)	BD (RVU)	FV (RVU)	SB (RVU)	P _{time} (min)	P _{temp} (°C)
Tray_45°C	362.17 ^e ±0.78	199.28 ^c ±0.63	162.89 ^c ±0.97	270.06 ^{cd} ±1.80	70.78 ^a ±1.17	4.62 ^b ±0.03	84.13 ^a ±0.02
Tray_55°C	362.72 ^e ±2.14	196.64 ^c ±2.35	166.08 ^{abc} ±0.76	268.64 ^d ±2.39	72.00 ^a ±2.38	4.60 ^b ±0.00	83.30 ^{bc} ±0.05
Tray_65°C	365.11 ^e ±3.21	199.28 ^c ±1.64	165.83 ^{abc} ±1.96	274.56 ^{bc} ±3.53	75.28 ^a ±2.04	4.62 ^b ±0.04	83.87 ^{ab} ±0.45
Infrared_45°C	373.75 ^{cd} ±2.64	206.31 ^b ±3.44	167.28 ^{abc} ±3.17	275.92 ^b ±1.47	69.61 ^a ±1.99	4.64 ^b ±0.04	83.57 ^{abc} ±0.42
Infrared_55°C	378.19 ^{abc} ±2.82	207.67 ^b ±2.19	170.53 ^{ab} ±3.97	278.31 ^b ±2.38	70.64 ^a ±2.76	4.51 ^a ±0.04	83.32 ^{bc} ±0.03
Infrared_65°C	380.47 ^{ab} ±7.19	208.39 ^b ±1.93	172.08 ^a ±7.50	278.36 ^b ±1.56	69.97 ^a ±3.42	4.62 ^b ±0.04	83.82 ^{ab} ±0.45
Fluidized_45°C	372.00 ^d ±0.78	207.42 ^b ±1.58	164.58 ^{bc} ±0.94	276.81 ^b ±2.02	69.39 ^a ±0.97	4.49 ^a ±0.03	83.00 ^c ±0.42
Fluidized_55°C	374.78 ^{bcd} ±3.75	219.17 ^a ±2.07	155.61 ^d ±1.68	287.78 ^a ±0.10	68.61 ^a ±2.15	4.62 ^b ±0.04	83.63 ^{ab} ±0.49
Fluidized_65°C	381.28 ^a ±2.84	218.31 ^a ±5.36	162.97 ^c ±7.28	288.64 ^a ±1.90	70.33 ^a ±4.66	4.62 ^b ±0.08	83.30 ^{bc} ±0.05

Notes: All values are means of three determinations. Values are means ± standard deviation. Within the same row, the values with different letters are significantly differently at p < 0.05 by LSD test. P_{temp} = temperature at which peak viscosity was reached; P_{time} = time from onset of pasting to peak viscosity; PV = peak viscosity; TV = trough viscosity; BD = breakdown; SB = setback, RVU = Rapid Visco-Analyzer unit.

Conclusions

The drying kinetics and effects of three drying methods namely tray, infrared and fluidized bed drying at 45, 55 and 65 °C on sweet potato starch were investigated. The results showed that the drying process took place only during the falling rate drying period for tray and infrared methods, but both constant and falling rate drying was found for fluidized bed drying. For tray drying, it took about 15, 8.5 and 5.5 h to get about 10 % final MC at 45, 55 and 65 °C respectively while to obtain the same MC at the same drying temperature, the drying time for infrared drying was 12, 6.5 and 4.5 h and for fluidized bed drying was 0.42, 0.28 and 0.2 h, respectively. All 11 drying models were suitable for describing SPS drying process due to high R^2 ($R^2 > 0.93$), and low in RMSE (0.002739 to 0.085240) and χ^2 (0.000003 to 0.007160). The Midilli model was found to be the best for explaining the starch drying behavior for all drying conditions. The effective diffusivity for fluidized bed drying was significantly higher than those in tray and infrared. The energy of activation in tray and infrared drying was nearly double the value of that in fluidized bed drying. The higher effective diffusivity or lower energy of activation, may result in the higher drying rate found. These drying conditions only slightly influenced the starch properties in terms of color, gel texture, swelling power, solubility and pasting properties. The drying rate would be the basis to select drying conditions, and due to the slightly inferior starch color dried by fluidized bed drying at 65 °C, the fluidized bed drying at 45 or 55 °C is recommended for sweet potato starch drying.

Acknowledgements

The authors thank the Food Engineering and Bioprocess Technology, Asian Institute of Technology, Thailand for supplying all needed equipment and thank the UNEP (United Nations Environment Program) Organization for financial support.

References

- [1] R Hoover. Composition, molecular structure, and physicochemical properties of tuber and root starches - a review. *Carbohydr. Polym.* 2001; **45**, 253-67.
- [2] SN Moorthy. Physicochemical and functional properties of tropical tuber starches - a review. *Starch-Starke* 2002; **54**, 559-92.
- [3] Z Chen. 2003, Physicochemical Properties of Sweet Potato Starches and Their Application in Noodle Products, Ph. D. Dissertation. Wageningen University, The Netherlands.
- [4] SMM Rahman. 2000, Extraction and Functional Properties of Different Varieties of Sweet Potato Starch, Ph. D. Dissertation. Asian Institute of Technology, Bangkok, Thailand.
- [5] W Liu and Q Shen. Studies on the physicochemical properties of mung bean starch from sour liquid processing and centrifugation. *J. Food Eng.* 2007; **79**, 358-63.
- [6] I Oduro, WO Ellis, S Acquah and F Kyerezateng. Solar and tray-drying methods and physicochemical properties of sweet potato starch. *Ghana J. Agric. Sci.* 2008; **41**, 100-10.
- [7] R Yadava, M Guhab, RN Tharanathan and RS Ramteke. Changes in characteristics of sweet potato flour prepared by different drying techniques. *Food Sci. Technol.* 2006; **39**, 20-6.
- [8] M Ahmed, MS Akter and JB Eun. Peeling, drying temperatures, and sulphite treatment affect physicochemical properties and nutritional quality of sweet potato flour. *Food Chem.* 2010; **121**, 112-8.
- [9] AZ Sahin, I Dincer, BS Yilbas and MM Hussain. Determination of drying times for regular multi-dimensional objects. *Int. J. Heat Mass Tran.* 2002; **45**, 1757-66.
- [10] M Maskan. Drying, shrinkage and rehydration characteristics of kiwifruits during hot air and microwave drying. *J. Food Eng.* 2001; **48**, 177-82.
- [11] GP Sharma, RC Verma and PB Pathare. Thin-layer infrared radiation drying of onion slices. *J. Food Eng.* 2005; **67**, 361-6.
- [12] R Khir, Z Pan, A Salim and JF Thompson. Drying characteristics and quality of rough rice under infrared radiation heating. In: An ASABE Meeting Presentation, ASABE Annual International Meeting. Minneapolis Convention Center, Minneapolis, Minnesota, USA. 2007.

- [13] S Soponronnarit, A Pongtornkulpanich and S Prachayawarakorn. Drying characteristics of corn in fluidized bed dryer. *Dry. Technol.* 1997; **15**, 1603-15.
- [14] HO Menges and C Ertekin. Thin layer drying model for treated and untreated Stanley plums. *Energ. Convers. Manage.* 2006; **47**, 2337-48.
- [15] EK Akpınar. Determination of suitable thin layer drying curve model for some vegetables and fruits. *J. Food Eng.* 2006; **73**, 75-84.
- [16] MGA Vieira and SCS Rocha. Mathematical modeling of handmade recycled paper drying kinetics and sorption isotherms. *Braz. J. Chem. Eng.* 2008; **25**, 299-312.
- [17] SP Ong and CL Law. Mathematical modeling of thin layer drying of salak. *J. Appl. Sci.* 2009; **9**, 3048-54.
- [18] EK Akpınar, Y Bicer and C Yildiz. Thin layer drying of red pepper. *J. Food Eng.* 2003; **59**, 99-104.
- [19] C Ertekin and O Yaldiz. Drying of eggplant and selection of a suitable thin layer drying model. *J. Food Eng.* 2004; **63**, 349-59.
- [20] M Kashaninejad, A Mortazavi, A Safekordi and LG Tabil. Thin layer drying characteristics and modeling of pistachio nuts. *J. Food Eng.* 2007; **78**, 98-108.
- [21] GD Singh, R Sharma, AS Bawa, and DC Saxena. Drying and rehydration characteristics of water chestnut (*Trapa natans*) as a function of drying air temperature. *J. Food Eng.* 2008; **87**, 213-21.
- [22] M Aghbashlo, MH Kianmehr and A Arabhosseini. Modeling of thin-layer drying of potato slices in length of continuous band dryer. *Energ. Convers. Manage.* 2009; **50**, 1348-55.
- [23] T Abe and TM Afzal. Thin-layer infrared radiation drying of rough rice. *J. Agr. Eng. Res.* 1997; **67**, 289-97.
- [24] S Tirawanichakul, W Naphatthalung and Y Tirawanichakul. Drying strategy of shrimp using hot air convection and hybrid infrared radiation/hot air convection. *Walailak J. Sci. & Tech.* 2008; **5**, 77-100.
- [25] SM Tasirin, SK Kamarudin, K Jaafar and KF Lee. The drying kinetics of bird's chillies in a fluidized bed dryer. *J. Food Eng.* 2007; **79**, 695-705.
- [26] T Madhiyanon, A Phila and S Soponronnarit. Models of fluidized bed drying for thin-layer chopped coconut. *Appl. Therm. Eng.* 2009; **29**, 2849-54.
- [27] American Association of Cereal Chemistries. *Approved Methods of the American Association of Cereal Chemistries.* 10th ed. The Association: St. Paul, Minn, 2000.
- [28] MAM Khraisheh, TJR Cooper and TRA Magee. The transport mechanism of moisture during air drying processes. *Food Bioprod. Process.* 1997; **75**, 34-40.
- [29] J Crank. *Chapter 1, 4, 10.* In: *The Mathematics of Diffusion.* 2nd ed. Clarendon Press, Oxford, London, 1975.
- [30] E Shimelis, M Meaza and S Rakshit. Physicochemical properties, pasting behavior and functional characteristics of flours and starches from improved bean (*Phaseolus vulgaris* L.) varieties grown in East Africa. *Inter. Comm. Agri. Eng.* 2006; **8**, 1-18.
- [31] M Pons and SM Fiszman. Instrumental texture profile analysis with particular reference to gelled system. *J. Texture Stud.* 1996; **27**, 597-624.
- [32] B Pankaj, GP Pathare and Sharma. Effective moisture diffusivity of onion slices undergoing infrared convective drying. *Biosystems Eng.* 2005; **93**, 285-91.
- [33] SSH Rizvi. *Thermodynamic Properties of Foods in Dehydration.* In: Rao MA and Rizvi SSH (eds.). *Engineering Properties of Foods.* New York: Marcel Dekker Inc., 1986, p. 190-3.
- [34] ZB Maroulis and DM Kouris. *Transport Properties in the Drying of Solids.* In: Mujumdar AS (ed.). *Handbook of Industrial Drying.* 3rd ed. Taylor and Francis Group, 2006.
- [35] J Shi, Z Pan, TH McHugh, D Wood, E Hirschberg and D Olson. Drying and quality characteristics of fresh and sugar-infused blueberries dried with infrared radiation heating. *LWT - Food Sci. Technol.* 2008; **41**, 1962-72.
- [36] HM Lai. Effects of hydrothermal treatment on the physicochemical properties of pregelatinized rice flour. *Food Chem.* 2001; **72**, 455-63.
- [37] M Ott and EE Hester. Gel formation as related to concentration of amylose and

- degree of starch swelling. *Cereal Chem.* 1965; **42**, 476-84.
- [38] LS Collado and H Corke. Properties of starch noodles as affected by sweet potato genotype. *Cereal Chem.* 1997; **74**, 182-7.
- [39] SY Lee, KS Woo, JK Lim, HI Kim and ST Lim. Effect of processing variables on texture of sweet potato starch noodles prepared in a nonfreezing process. *Cereal Chem.* 2005; **82**, 475-78
- [40] P Malumba, S Janas, O Roiseux, G Sinnaeve, T Masimango, M Sindic, C Deroanne and F Bera. Comparative study of the effect of drying temperatures and heat-moisture treatment on the physicochemical and functional properties of corn starch. *Carbohydr. Polym.* 2010; **79**, 633-41.
- [41] HD Belitz, W Grosch and P Schieberle. *Chapter 4. In: Food Chemistry.* 4th ed. Springer-Verlag Berlin Heidelberg, Germany, 2009.